HHS Public Access

Author manuscript

Trends Analyt Chem. Author manuscript; available in PMC 2016 December 19.

Published in final edited form as:

Trends Analyt Chem. 2016 November ; 83(A): 53–64. doi:10.1016/j.trac.2016.04.020.

Compact NMR relaxometry of human blood and blood components

David P. Cistola[a,b,*] and **Michelle D. Robinson**[a,b]

[a]Nanoparticle Diagnostics Laboratory, Institute for Cardiovascular and Metabolic Diseases, University of North Texas Health Science Center, Fort Worth, Texas 76107, USA

[b]Departments of Clinical Laboratory Science and Biochemistry & Molecular Biology, College of Allied Health Sciences and Brody School of Medicine, East Carolina Diabetes & Obesity Institute, East Carolina University, Greenville, North Carolina 27834, USA

Abstract

Nuclear magnetic resonance relaxometry is a uniquely practical and versatile implementation of NMR technology. Because it does not depend on chemical shift resolution, it can be performed using low-field compact instruments deployed in atypical settings. Early relaxometry studies of human blood were focused on developing a diagnostic test for cancer. Those efforts were misplaced, as the measurements were not specific to cancer. However, important lessons were learned about the factors that drive the water longitudinal (T_1) and transverse (T_2) relaxation times. One key factor is the overall distribution of proteins and lipoproteins. Plasma water T_2 can detect shifts in the blood proteome resulting from inflammation, insulin resistance and dyslipidemia. In whole blood, T_2 is sensitive to hemoglobin content and oxygenation, although the latter can be suppressed by manipulating the static and applied magnetic fields. Current applications of compact NMR relaxometry include blood tests for candidiasis, hemostasis, malaria and insulin resistance.

Keywords

Nuclear magnetic resonance; Relaxometry; T_1 and T_2; Relaxation times; Plasma; Serum; Blood cells; Malaria; Candidiasis; Hemostasis; Insulin resistance

1. Introduction

Nuclear magnetic resonance (NMR) encompasses a family of diverse methods and can be divided into three broad categories: spectroscopy, imaging and relaxometry. The early history of NMR is rooted in spectroscopy, as chemical shift resolution has enabled chemists and structural biologists to deduce the structures of increasingly complex molecules. Since the 1980's, the medical community has been exploiting the spatial resolution afforded by magnetic resonance imaging (MRI) to inform diagnosis and therapy. Thus, the core strengths

*Corresponding author. Tel.: +1 8177352055; Fax: +1 8177350254., david.cistola@unthsc.edu (D.P. Cistola).

of spectroscopy and imaging are atomic and spatial resolution, respectively. However, both approaches can be used to study nuclear spin relaxation properties as well, yielding the spin-lattice (T_1) and spin-spin (T_2) relaxation time constants.

The term relaxometry refers to a class of NMR experiments whose primary emphasis is on measuring nuclear spin relaxation times, with the goal of characterizing the physical and dynamical properties of a sample. One of the best kept secrets in NMR is that relaxation analyses can be performed *without* spectroscopy or imaging. Although this approach sacrifices the power of atomic or spatial resolution, it has three key attributes: *portability, simplicity and cost*. These features enable NMR technology to penetrate new settings, well beyond the specialized NMR laboratory or imaging center. Benchtop or portable NMR devices, about the size of a laser printer, are being deployed in agricultural field sites to assess the moisture content of seeds, or on food production lines for quality control [1]. Compact NMR devices are being lowered deep into underground oil wells for exploration and data logging [2]. And the NMR MOUSE, a miniature one-sided NMR device, is being used for *in situ* non-destructive testing of human skin, historical paintings and other materials [3,4].

Unlike spectroscopy, where chemical shift resolution often hinges on the use of high-field superconducting magnets with homogeneous B_o fields, relaxometry can be performed using low-field permanent magnets with relatively inhomogeneous fields. A variety of benchtop, portable or compact instruments have been designed for this purpose. These instruments have magnetic fields of 0.1 to 1.5 Tesla, corresponding to ^1H resonance frequencies of approximately 5–60 MHz: one-to-two orders of magnitude lower than the conventional NMR spectrometers used in chemistry laboratories. In addition, low-field relaxometry is forgiving with respect to sample type. Unlike NMR spectroscopy, which depends on narrow linewidths, relaxometry readily accommodates semi-solid or liquid crystalline samples. It can be used with heterogeneous samples such as seeds, crude oil, polymers, yogurt, and even whole animals for body composition analysis.

The petroleum, agriculture and food industries were among the first to embrace compact NMR relaxometry and have used it to solve a variety of practical problems in field exploration, production and quality control. In addition, the imaging community has used it to evaluate contrast agents and to optimize other aspects of image contrast in MRI. As described below, NMR relaxometry has been successfully implemented for several blood-based diagnostic tests, and additional applications are being explored.

Over the last few decades, compact NMR technology has held a back seat to the explosive developments in high-field spectroscopy and imaging. More recently, that order has been changing. There is a growing recognition that a number of important problems can be solved by NMR without the need for high-end spectroscopy or imaging. The portability, simplicity and low cost open up exciting new avenues and opportunities for NMR.

The purpose of this article is two-fold: (1) to review how NMR relaxometry has, and is, being applied to the analysis of human blood and blood components, and (2) to discuss future prospects for compact relaxometry-based blood tests for clinical diagnosis and

population health screening. Blood is a complex, heterogeneous mixture containing many hundreds of proteins and metabolites, as well as lipoprotein nanoparticles, cell-derived microparticles, blood cells, and an abundance of water. The challenge is to extract meaningful health-related information from complex samples, using simple but sound analytical approaches.

2. Methods used in compact NMR relaxometry

The primary methodological distinction of low-field NMR relaxometry is that data are analyzed in the time-domain, rather than the frequency domain. In spectroscopy and imaging, the raw time-domain signal is Fourier transformed to generate a frequency-domain format. For spectroscopy, this calculation yields a spectrum of peaks, each containing information about resonance frequency (recorded as the chemical shift), as well as amplitude and phase. Using the proper pulse sequences, relaxation times can be extracted by analyzing the decay or recovery of the amplitudes of the frequency-domain peaks as a function of delay time.

By contrast, in relaxometry, the raw time-decay signal is analyzed without Fourier transformation. No spectra are generated, and no chemical shifts are recorded. Rather, the relaxation times are obtained by analyzing the exponential decay or recovery of the *time-domain* NMR signal. Although atomic resolution is sacrificed, the T_1 or T_2 relaxation times have some resolving power of their own [5]. Relaxation times are sensitive to rotational and translational diffusion, as well as chemical exchange processes. Thus, multi-component or multi-phase samples may contain resolvable domains with distinctly different T_2 or T_1 values. Examples include solutions containing large molecules along with much smaller ones, e.g., proteins dissolved in an aqueous buffer. Another example is an aqueous suspension of lipid emulsions, such as found in dairy products or in blood, where the dynamics of the emulsified lipid molecules are considerably different from those in the aqueous phase. A third example includes molecules that contain distinct mobility domains, such as long-chain substituted hydrocarbons in oil or liquid crystalline phases.

The methods used to acquire data in compact NMR relaxometry are variations of the experiments used in spectroscopy and imaging. For lucid descriptions of relaxation experiments, the reader is referred to the books by James [6], Freeman [7], and Levitt [8]. Inversion-recovery is used to acquire T_1; Hahn spin-echo and Carr-Purcell-Meiboom-Gill (CPMG) experiments are used to measure T_2. Spin-lock experiments can be used to determine the rotating-frame relaxation time $T_{1\rho}$. If quantitation of T_1 or T_2 is not required, simpler experiments can be devised to compare the time-domain free-induction decay patterns of different samples.

Another class of relaxometry experiments monitor relaxation dispersion, the magnetic field dependence of relaxation times. The field dependence of T_1, T_2 and $T_{1\rho}$ offer insights into the mechanisms that contribute to nuclear spin relaxation. Some of these experiments utilize specialized hardware for fast-field-cycling NMR [9].

Although the inversion recovery and Hahn spin echo experiments have important roles in relaxometry, the CPMG experiment is the method of choice for analyzing and resolving multi-component systems. Beyond its ability to suppress the effects of magnetic field inhomogeneity and other artifacts, it offers the quickest, most robust way to record a well-sampled exponentially decaying signal with a high signal-to-noise ratio. These requirements are critical for detecting and resolving the weaker, non-water signals in plasma, serum and blood, but also are important for obtaining accurate water relaxation times.

A modified CPMG pulse scheme for NMR relaxometry developed by our laboratory is shown in Fig. 1. Four features of this pulse sequence warrant further explanation:

1. *Water suppression*: The composite 180° pulse ($90_x180_y90_x$) and Δ delay was introduced prior to the CPMG scheme to partially suppress the water signal and eliminate radiation damping. Radiation damping is the additional torque on the spin system generated by the intense water magnetization [7], and it varies with sample size, field strength and probe design. It can be detected as a non-exponential artifact in the calculated residuals of the exponential fit. Using the residuals as a guide, the Δ delay can be tuned to eliminate radiation damping while retaining as much water signal as possible to enhance signal-to-noise ratio. If the residuals show oscillations or other non-random deviations from zero, the delta delay is shortened until the residuals appear random. This approach to partial water suppression differs from high-field NMR spectroscopy, where the usual goal is to achieve essentially complete water suppression.

2. *Delayed acquisition*: Relaxation experiments for plasma, serum and blood samples generate several exponential decay components, and too many components creates challenges with multi-exponential analysis. We introduced an optional delayed acquisition, or DA loop, to eliminate the most rapidly decaying components, i.e., the ^1H nuclei of large proteins or protein assemblies. This facilitates the analysis of the slower decaying components from mobile lipid and protein domains, and from water. In most of our experiments with blood components, the DA loop is set to eliminate the first 19 msec of the exponentially decaying signal.

3. *180 pulse optimization*: The 180° pulses in the CPMG loops are phase alternated to cancel artifacts resulting from pulse imperfections [10]. In addition, the first 180° used for water suppression is executed as a composite $90°_x$-$180°_y$-$90°_x$ in order to improve performance [11].

4. *Data sampling control*: The adjustable DE loop determines how frequently the spin echo intensities are acquired. Such control becomes important if the goal is to maintain uniform sampling while varying 2τ, the delay time between successive 180° pulses in the CPMG scheme. It is also important for adjusting data sampling for decay curves with a wide range of T_2 values.

The 2τ inter-pulse delay impacts the effective CPMG field strength and is an important determinant of the T_2 value in blood samples [12]. Variation of CPMG field strength can be used in relaxation dispersion experiments to estimate chemical exchange rates, as has been demonstrated with protein NMR spectroscopy [13]. Also, short 2τ values are necessary to suppress contributions to T_2 resulting from the translational diffusion of molecules in an inhomogeneous field [14]. Inhomogeneous magnetic fields are common with the low-field permanent magnets used in compact relaxometers, which lack shim coils. For a particular instrument, the influence of translational diffusion at a given temperature can be assessed by collecting a series of CPMG experiments with increasing 2τ values. The sample should be one where chemical exchange contributions to T_2 are negligible or absent, such as pure water. Many of the early blood sample studies described below used relatively long 2τ delays (greater than ~1 ms), so it is possible that instrument-specific diffusion effects may have contributed in part to the observed study-to-study variations in T_2.

The absence of the Fourier transform in CPMG relaxometry provides two key advantages: high data sampling and quick data acquisition. In spectroscopy, it is customary to collect an array of 10–40 spectra, each acquired with a different total CPMG decay time, i.e., the total time allowed for partial signal decay during CPMG. In relaxometry, the entire CPMG decay curve is acquired in just one data set. Because of this advantage, the relaxometry curve can contain hundreds-to-thousands of time points rather than just 10–40. The high data sampling rate is necessary for a robust deconvolution of multi-exponential decay curves. A highly-sampled, eight-scan CPMG relaxometry experiment on human blood serum can be collected in just 3–4 minutes. The short data collection time is critical for the translation of NMR into clinical diagnostic settings, where high sample throughput is necessary to keep testing costs down.

For mono- or bi-exponential T_1 or T_2 decay curves, the analysis and extraction of relaxation times is straight forward. A bigger challenge lies in analyzing curves with three or more exponential terms. An inverse Laplace transform can be used to extract time constants and amplitudes for multi-exponential decay curves. These algorithms are implemented in programs such as CONTIN [15] and XPFIT [16]. The XPFIT program permits the user to choose a continuous or discrete analysis and to constrain the number of exponential terms in the latter. While powerful and useful, caution is warranted when performing inverse Laplace calculations. For scientists used to Fourier transforms of raw NMR data, the inverse Laplace calculation is not nearly as stable and robust [17]. If the data is noisy, the inverse Laplace calculation may represent an ill-posed problem [18]. The key to achieving robust inverse Laplace analysis is to ensure that the raw CPMG decay curves have high signal-to-noise ratios and are free of non-exponential artifacts. With aqueous samples like blood plasma, achieving high signal-to-noise for quantifying water T_2 is not difficult. However, if the goal is to quantify the T_2 values for the *non*-water components of blood (proteins, lipids, etc.), extensive signal averaging is often necessary.

For quick 8- or 16-scan data acquisitions for human plasma or serum samples using the pulse sequence in Fig. 1, we find that stable and reproducible discrete inverse Laplace fits can be obtained with three exponential terms. Three is the minimum number needed to obtain random residuals. For longer runs with 256-to-2048 scans, four exponential terms can

be used, as the increased signal-to-noise adds information content to the data. For concentrated samples such as oil-phase lipids, four-term fits can be used, as illustrated below.

When using discrete inverse Laplace transforms to compare plasma, serum or blood samples across a cohort of human subjects, it is important to fix the number of exponential terms to the same number in order to obtain a valid “apples-to-apples” comparison. The discrete algorithm in the XPFIT program is useful for this purpose, as it allows user control over the number of exponential terms, with a maximum of four.

A sample CPMG decay curve, recorded for sample of blood serum from a healthy human subject, is illustrated in Fig. 2A. Unlike the conventional NMR free-induction decay, this is a pure exponential decay curve containing no frequency oscillations. A T_2 profile with four peaks, obtained by continuous inverse Laplace transformation in CONTIN, is shown in Fig. 2B. This T_2 profile superficially resembles a NMR spectrum, but has a different x-axis (time rather than frequency) and a fundamentally different meaning. The large blue peak on the right, centered at ~800 msec, represents the T_2 distribution for water in human serum. The area under that peak provides the relative amplitude of that exponential component. In addition, the profile reveals three small orange peaks on the left, corresponding to T_2 distributions for protons in mobile lipid and protein domains. This particular data set was acquired with 2048 scans in order to have sufficient signal-to-noise to tease out those much smaller components. While the continuous T_2 profile is helpful for visualizing the distribution of T_2 values, we employ the discrete algorithm in XPFIT for T_2 quantification.

Fig. 2C shows the superimposition of water peaks obtained for serum samples from 29 asymptomatic, apparently healthy human subjects, illustrating the significant person-to-person variability in serum water T_2. The source of this variability is a major focus of our current research [19].

3. Low-field relaxometry studies of the liquid components of blood

Many of the water relaxometry studies of samples containing proteins and other blood components were motivated by an interest in defining the factors that affect image contrast in MRI. Relaxation times are heavily exploited in imaging, as exemplified by the schemes for recording T_1- and T_2-weighted images. Some low-field relaxometry studies have been performed using whole-body MRI instruments, which are hardly compact. Nevertheless, those results provide fundamental insights into the factors that drive relaxation times and offer a glimpse into the potential for compact relaxometry studies of blood products.

By mass, water accounts for >80% of blood and >90% of blood serum or plasma. Therefore, water yields the dominant ^{1}H NMR signal (Fig. 2B). Water molecules form hydrogen bonds with virtually every protein, lipoprotein and metabolite in the blood. Thus, the relaxation properties of water can be used to monitor the type and relative quantities of blood proteins and lipoproteins.

In low-field relaxometry, it is possible to detect the lipid and protein components directly, not via water (Fig. 2B, inset). However, that approach requires more care in the collection of

data and has rarely been used. Therefore, most of the low-field relaxometry studies discussed in this review monitor blood components *via* the spin relaxation of the water ^{1}H NMR signal.

In Section 3, we begin by discussing the liquid components of blood: fractionated serum and plasma proteins, lipids and lipoproteins, followed by unfractionated whole plasma and serum. Section 4 addresses studies of blood cells and whole blood.

3.1. Serum and plasma proteins

Proteins are highly concentrated in blood serum (6.1–8.1 g/dL) and plasma (6.4–8.4 g/dL), with fibrinogen concentration essentially making up the difference between the two. While there are hundreds of proteins in blood plasma, the ten most abundant proteins (albumin, IgG, transferrin, fibrinogen, IgA, α2-macroglobulin, IgM, α_1-antitrypsin, C3 complement and haptoglobin) account for over 90% of the total protein concentration, and the top two, nearly 80% [20]. Therefore, a relatively small number of proteins and lipoproteins are the dominant effectors of water T_1 and T_2 relaxation in serum and plasma.

An important observation is that water relaxation rates are linearly correlated with protein concentration, irrespective of the protein type [21–24]. This is a consequence of several factors. Water relaxation is modulated by Brownian molecular motions. It results from fluctuating local fields and is governed largely by the dipole-dipole relaxation mechanism [6]. The ^{1}H T_1 and T_2 values for protein-bound water molecules in solution are inversely proportional to the correlation time for rotational diffusion of the protein-water complex, i.e., the time it takes for the ^{1}H magnetic dipoles to rotate by one radian in the static magnetic field of the NMR instrument. In turn, the rotational correlation time depends on temperature and viscosity, as defined by the generalized Stokes-Einstein-Debye equation [25,26] which is reproduced in ref. [5]. The protein-bound water molecules (treated as solute in the Stokes-Einstein-Debye analysis) rotate at the much slower reorientation rate of the protein; thus, the *observed* water T_1 and T_2 values in protein solutions are lower than those of unbound water [27]. In addition, the protein-bound water molecules undergo ^{1}H exchange with unbound water and with the hydrogen atoms on ionizable groups of the protein. These exchange processes can further decrease the observed ^{1}H T_2 value for water [28,29]. Taken together, water relaxation times are influenced by the binding and exchange of water molecules on and off protein binding sites, as well as sample viscosity.

The dominant terms contributing to water relaxation rate constants are given in Equations (1) and (2). Here, $R_{1dd,free}$ and $R_{2dd,free}$ represent the dipolar relaxation rates for free, unbound water; $R_{1dd,bound}$ and $R_{2dd,bound}$ represent the dipole-dipole relaxation rate constants for protein-

$$1/T_1 = R_1 = R_{1dd,free} + R_{1dd,bound} + R_{1ed,paramagnetic} \quad (1)$$

$$1/T_2 = R_2 = R_{2dd,free} + R_{2dd,bound} + R_{2,exchange} + R_{2,diffusion} + R_{1ed,paramagnetic} \quad (2)$$

bound water; and $R_{2,exchange}$ and $R_{2,diffusion}$ represent the contributions of chemical exchange and diffusion to R_2 relaxation rates, respectively. The remaining terms represent the electron-dipole relaxation resulting from paramagnetic centers.

The ^1H on/off exchange rates for water (sub-nsec) are fast relative to the T_1 and T_2 time scales (msec-sec). Therefore, protein-bound and unbound water yield a weighted-average T_1 or T_2 value. As protein concentration increases, the fraction of bound water increases and the exchange-averaged relaxation time decreases.

The contributions of individual proteins to water relaxation can be compared using plots of water relaxation rates *vs.* protein concentration. The slope of R_1 or R_2 *vs.* protein concentration is defined as the *relaxivity*, a measure of a protein's effect on water ^1H relaxation per unit protein concentration. Relaxivity values for a number of human blood proteins and protein fractions are listed in Table 1. Note that albumin, one of the lower molecular weight proteins in blood, has the lowest relaxivity values among this group. In general, relaxivity values increase with molecular weight. For example, the γ-globulin fraction contains a significant fraction of IgM, the largest protein in blood, and IgG, which has over twice the molecular weight of albumin. The highest relaxivity was observed with transferrin, a protein that binds paramagnetic iron and has a disproportionately large impact on water relaxation. Except for transferrin, the R_2 relaxivity values are much higher than those for R_1, indicating that R_2 is much more responsive to changes in protein concentration. That occurs, in part, because the transverse relaxation of water in protein solutions can be influenced by additional factors (translational diffusion and/or chemical exchange) that normally do not contribute to R_1. Knowing the relaxivity values under matched conditions, one could predict the impact of changes in the concentration of individual proteins or protein fractions on T_2 or T_1.

Fig. 3 plots T_2 as a function of total protein concentration for purified albumin (triangles), lipoprotein-deficient serum (squares), and whole serum (circles). This plot roughly spans the range of albumin and total protein concentration found in human serum. The observed differences for these three fractions highlight the disproportionately large impact of non-albumin proteins and lipoproteins on water T_2 values. The apparent linearity is a consequence of the relatively narrow range of protein concentrations examined. When the albumin plot includes protein concentrations well below 3 g/dL, it takes on the expected hyperbolic shape of a reciprocal function.

Note that the curves in Fig. 3 are not relaxivity plots, as the y-axis is T_2 rather than R_2. When the data are recast as R_2, the plots are linear and the slopes differ in the following order: albumin < lipo-protein-deficient serum < whole serum. This provides further evidence that the non-albumin proteins and lipoproteins – collectively termed globulins – have higher relaxivity values compared with albumin. Thus, an increase in the globulin/albumin ratio, as can occur in the human circulation, would be predicted to lower serum water T_2. An inverse

correlation between serum or plasma T_2 and globulin concentration or globulin/albumin ratio has been observed in studies of human subjects [19].

Another important consideration in protein relaxometry is the dependence of relaxation times on B_o field strength [30]. Early relaxation dispersion studies of serum albumin at different concentrations and temperatures suggested three rapidly-exchanging pools of water: free, translationally restricted, and rotationally bound [31]. Monitoring the temperature dependence of T_1 values, thermodynamically structured water was observed to have different properties in human albumin *vs.* γ-globulins [32]. Studies using ^2H and ^{17}O relaxation dispersion revealed that protein water T_1 relaxation in protein solutions is heavily influenced by a relatively small number of tightly bound or buried water molecules that undergo rotational motions with the protein [33,34].

An important observation for low-field NMR is that water T_2 (unlike T_1) varies little with B_o, at least over the 5–60 MHz range of field strengths typically encountered in compact NMR instruments.

3.2. Lipids and lipoproteins

Human blood contains several classes of lipid-rich nanoparticles termed plasma lipoproteins. The function of these particles is to transport insoluble cholesteryl esters and triglycerides through the circulation, and to target their lipid cargo to particular tissues and metabolic pathways. The plasma lipoproteins are categorized by density and consist of four main classes: low-density lipoprotein (LDL), high-density lipoprotein (HDL), very-low density lipoprotein, (VLDL) and chylomicrons (CM).

The general architecture of the particles consists of an oil-phase lipid core surrounded by a monolayer of amphiphilic phospholipids, un-esterified cholesterol and proteins [35,36]. The LDL and HDL particles have a cholesteryl ester-rich core, with considerably less triglyceride. By contrast, VLDL and CM have a predominately triglyceride-rich core. The physical and biological properties of the phospholipid, cholesteryl ester and triglyceride components are heavily influenced by their constituent fatty acids, which vary in hydrocarbon chain length and degree of unsaturation.

Lipoprotein particles are remodeled during metabolism and disease. For example, insulin resistance and diabetes causes LDL and HDL to become more triglyceride rich, altering their uptake and clearance from the blood. Moreover, the fatty acid compositions of the particles are altered by diet and metabolism, resulting in changes in molecular motions and lipid fluidity.

Compact NMR relaxometry is well suited to track the remodeling of lipoproteins in metabolism and disease. Initial work was performed using oil-phase lipids and mixtures designed to mimic some aspects of the lipoprotein core [5]. Fig. 4 displays the T_2 profiles for a series of pure 18-carbon fatty acids that vary in the number and position of double bonds. Using an inverse Laplace transform to analyze the multi-exponential decay curves, three distinct T_2 components were resolved. These components were assigned to clusters of protons in segments of the hydrocarbon undergoing distinct motions. Large shifts in T_2

values were seen with increasing numbers of *cis*-double bonds. The ^{1}H T_2 values for oil-phase fatty acids are sensitive to lipid fluidity which, in turn, is governed by molecular packing [5]. This is further illustrated by the variation with hydrocarbon chain length and double bond stereochemistry (Fig. 2 of ref. [5]). In addition, T_2 differences can be detected for lipid mixtures that mimic the serum fatty acid compositions of individuals on diets rich in saturated, mono-unsaturated or polyunsaturated fats (see fig. 5 of ref. [5]).

While elegant analyses have been conducted using high-resolution NMR spectroscopy [37], there are virtually no reports using compact relaxometry to characterize plasma lipoproteins. The data from lipid model systems demonstrates the resolving power of T_2 with respect to lipid mobility domains [5], which may be achievable with lipoproteins as well. Benchtop relaxometry studies of the lipid and protein ^{1}H signals from lipoprotein fractions, as well as lipoproteins in whole serum, are ongoing in our laboratory and will be reported elsewhere.

3.3. Whole plasma and serum

Blood plasma and serum are related but distinct liquid fractions of the blood. Serum is obtained after waiting for the blood to clot in the collection tube, and then separating the fibrin clot and blood cells from the liquid supernatant by low-speed centrifugation. By contrast, plasma is obtained by centrifuging whole blood collected using a tube that contains an anti-coagulant. Thus, serum and plasma are not equivalent and have distinct protein compositions and concentrations [20]. Plasma contains five clotting factor proteins not present in serum, namely factors I, II, V, VIII and XIII. All but one have low concentrations, but factor I (fibrinogen) is abundant, constituting approximately 4% of total plasma protein. Plasma fibrinogen levels correlate inversely with plasma water T_2 relaxation times [23].

Water ^{1}H relaxation times for human plasma and serum, recorded by different laboratories under a range of conditions, are compiled in Table 2. The results are listed in order of increasing magnetic field strength. Four main observations can be made. First, T_2 values are consistently lower than those for T_1. The correlation co-efficient between T_1 and T_2 values, measured by the same laboratory under comparable conditions, is approximately 0.6 [38]. Compared with T_1, water T_2 relaxation includes additional contributions from low-frequency fluctuations such as slow rotational motions, chemical exchange and diffusion [6–8], so there is a conceptual basis for the divergence of T_1 and T_2 observed with plasma samples. A second observation is that T_1 values increase with B_o magnetic field strength, consistent with dipole-dipole relaxation being the dominant contributor to T_1. By contrast, T_2 shows little or no dependence on B_o field under these conditions. Third, the T_2 values obtained with short CPMG 2τ delays below 1 ms [19,23] are noticeably higher than those obtained with longer 2τ delays. This observation is consistent with the concept that higher effective CPMG field strength suppresses contributions to T_2 from exchange and diffusion. Fourth, the T_1 or T_2 values appear to differ in some groups of healthy individuals compared those with certain metabolic abnormalities or diseases. This observation is discussed further in Section 3.4.

As with purified protein solutions, the relaxation rates of water in human plasma or serum are influenced by the binding and exchange of water ^{1}H with the largest and most abundant proteins and lipoproteins. In addition, human plasma and serum contains a number of low

molecular weight metabolites that can interact with water, such as glucose and amino acids. However, water-metabolite interactions are expected to have a negligible influence on the relaxation times of water, mainly because dipolar relaxation is inefficient for low molecular weight compounds. This prediction is supported by our *in vitro* studies of water T_2 *vs.* metabolite concentration over ranges relevant to human physiology. An exception occurs at very high concentrations of glucose (>250 mg/dL), which occurs *in vivo* only in severe, uncontrolled diabetes. Under these conditions, glucose reacts non-enzymatically with protein side chains, forming Schiff-base adducts and advanced glycation end products that can enhance the binding of water to proteins.

Overall, water T_1 and T_2 values are strongly influenced by the *total* serum or plasma protein concentration, as well as the *relative amounts* of individual protein and lipoproteins [19,23]. High molecular weight proteins are predicted to have a disproportionately large influence on relaxation times [39]. In addition, proteins that have larger numbers of tightly bound waters are expected to have a greater influence on relaxation times. Both of these factors are captured in the relaxivity value for each protein.

The observed R_1 or R_2 value for a given serum or plasma sample can be estimated by summing the individual contributions of the most abundant protein and lipoprotein components:

$$R_i(\text{obs}) = c_1 r_{i1} + c_2 r_{i2} + c_3 r_{i3} + \dots \quad (3)$$

Here, c_1 and r_1 represent the concentration and relaxivity of the first protein or protein class, and $i = 1$ or 2 for R_1 or R_2, respectively. To first approximation, such estimates come close to values for whole plasma or serum [21–24]. This analysis depends on having accurate relaxivity values for each protein and lipoprotein class, measured under an appropriately matched set of experimental conditions.

3.4. Plasma and serum relaxometry and human disease

The early literature relating plasma or serum water ^1H relaxation times to human disease was characterized by initial excitement that soon led to controversy. In the 1970's and 80's, there was a flurry of interest in the possibility of using NMR relaxometry as a blood test for early cancer detection [23,38–43]. The efforts in humans were stimulated by prior results in animals showing an increase in T_1 for tumors as compared with normal tissues [44,45] as well as a "systemic effect": an increase in the T_1 for the serum of animals developing cancer [46–48]. Subsequent studies in humans yielded mixed results and interpretations. Several groups observed an increase in plasma or serum T_1 in cancer patients [38,41–43], while others saw no significant difference [22,23,39,40]. The relaxation times measured in these studies are cataloged in Table 2. In the end, it was determined that the observed changes in relaxation times were not specific to cancer *per se*, but reflected the host's response to the disease. The initial enthusiasm surrounding a possible blood test for cancer gave way to some disillusionment and skepticism about using NMR relaxometry as a clinical diagnostic tool [22].

In spite of the disappointment regarding cancer, some important lessons were learned along the way. First, the *total* protein concentration and the *relative distribution* of proteins are among the most important physiological factors driving plasma and serum relaxation times. As expected from the dipolar contributions to relaxation, larger molecular weight proteins have a disproportionate effect, especially on lowering T_2 values (Table 2 and refs. [23,39]). The contributions from individual proteins are additive: the observed relaxation times for whole plasma or serum can be estimated by summing up the (concentration * relaxivity) terms for the main protein fractions [21–23,39]. Endogenous paramagnetic ions in human serum appear to have a negligible impact [21,49].

A second lesson learned was that plasma relaxation times are influenced by viscosity as well. Protein concentration and viscosity are highly correlated. After correcting for total protein concentration, approximately 40%–60% of the variation in plasma T_2 could be explained by variations in viscosity [23]. A third lesson was that T_2 is more sensitive to protein and viscosity shifts than is T_1, when results are compared under controlled conditions and short 2τ values are used [19,23]. Much of the early efforts to correlate relaxation times with disease were based on T_1 results only [40,42,50].

Rather than cancer, a more promising clinical application of plasma or serum T_2 measurements is in monitoring disease states more closely associated with shifts in blood proteins and lipoproteins. One such shift occurs in the acute phase response to infection or injury. The acute phase response is a component of innate immunity, the body's first line of defense against invading microorganisms. The liver increases its secretion of some proteins into the circulation (positive acute phase reactants) while decreasing others. As albumin is a negative acute phase reactant and is abundant in plasma and serum, the net shift in the acute phase response is toward higher molecular weight proteins. Indeed, T_2 is significantly lower in diseases characterized by inflammation or infection (Table 2 and refs. [23]). Though possible, it is impractical in the routine evaluation of a clinic patient to measure a panel of individual proteins, chemokines and cytokines in order to monitor the acute phase response. Unlike biomarker panels, the water T_2 values provide a high-level view of shifts in the blood proteome in just one measurement. No existing diagnostic or screening test provides such a perspective on human physiology or pathology.

A more subtle form of inflammation occurs with the early metabolic abnormalities that precede type 2 diabetes [51,52]. Since the 1980's, the prevalence of diabetes has been skyrocketing and has become a major threat to the health and well being of societies world wide [53]. Conventional measures for screening and prevention occur too late, as glucose or hemoglobin A_{1c} levels do not become abnormal until over half of pancreatic insulin secretory capacity has been irreversibly lost [54]. Thus, there is a need for practical methods that detect diabetes and prediabetes risk at an earlier stage. Preliminary results indicate that plasma T_2 is sensitive to the early insulin resistance and metabolic inflammation that precede prediabetes, metabolic syndrome and overt diabetes [19]. This is an active area of investigation by our laboratory, and additional results are forthcoming.

Another recent and exciting application of compact NMR relaxometry is in the rapid diagnosis of infectious diseases such as Candidiasis. By exploiting magnetic nanoparticles

coupled with specific antibodies, low levels of infectious agents can be detected using benchtop T_2 measurements [55,56]. Related technology is being developed for the clinical evaluation of hemostasis, namely disorders of clotting and bleeding [57]. These new applications of compact NMR relaxometry are the focus of another article in this issue authored by Thomas J. Lowery.

4. Low-field relaxometry of whole blood and blood cells

4.1. Factors affecting relaxation times in whole blood and blood cells

In whole blood, water exists in at least two distinct compartments: intracellular and plasma. The red blood cells outnumber white blood cells by a factor of 1000 and platelets, by a factor of ten. Moreover, red cells have five times the diameter and considerably more volume than platelets. Therefore, the intracellular water compartment for whole blood is dominated by the hemoglobin-rich environment inside of red blood cells. The intracellular hemoglobin concentration, clinically measured as the mean corpuscular hemoglobin concentration, is 32–36 g/dL: 4–5 times the total protein concentration in plasma. From protein binding and viscosity considerations alone, it follows that the water T_1 and T_2 values for the intracellular compartment should be significantly lower than those for plasma. Indeed, the reported water relaxation times for whole blood are lower than those for plasma. For example, the water T_1 values at 20 MHz and 37°C are approximately 900–1100 ms for whole blood as compared with 1400–1500 ms for plasma. Likewise, the T_2 values are ~300–500 ms lower in whole blood as compared with plasma (Tables 2 and 3).

Another consequence of the two distinct compartments is the asymmetric distribution of paramagnetic heme iron. Oxygenated hemoglobin, abundant in the red blood cells of arterial blood, is diamagnetic. However, the deoxygenated forms abundant in venous blood are paramagnetic. This paramagnetism results in a magnetic susceptibility difference between the blood cell and plasma compartments, generating local field gradients that dephase water coherence as it diffuses through those gradients. Thus, ^{1}H water T_2 decreases as the fraction of deoxy-hemoglobin increases. This phenomenon was first described by Thulborn and colleagues in 1982 [58] and has been the focus of intensive study since then [59–68]. Moreover, the paramagnetic deoxy-hemoglobin effect on T_2 has been exploited by Ogawa and colleagues to achieve blood oxygen-level dependent (BOLD) contrast in MRI [69]. The BOLD technique has become the mainstay of functional MRI, which revolutionized the field of brain activity mapping [70,71]. An interesting personal and historical account of these discoveries was published by Thulborn in 2012 [72].

The deoxy-hemoglobin gradient diffusion phenomenon in whole blood affects T_2 but not T_1, as diffusion is not a relaxation mechanism for T_1. The magnitude of the effect increases with $(B_o)2$, with a quadratic dependence of T_2 on the fraction of deoxygenated hemoglobin in blood [58,66,68]. The effect can be suppressed by shortening the 2τ delay between successive 180° pulses in the CPMG scheme (Table 3 and refs. [58,59,66,68]). It becomes insignificant at B_o fields below ~1 T or 43 MHz for 1H when 2τ is less than a few msec. Moreover, the effect depends on deoxy-hemoglobin being sequestered in an intracellular compartment and can be eliminated by lysing the red blood cells (Table 3 and refs. [58,59]).

A related, but distinct paramagnetic phenomenon affects *both* T_1 and T_2 in whole blood. The met-hemoglobin form of deoxy-hemoglobin contains a Fe(III) center, which permits a close proximity of water in the first hydration shell, leading to efficient electron-nucleus dipolar relaxation [58,61]. Both T_1 and T_2 are lowered, but the effect may be more pronounced in T_1 as it represents a larger percent contribution to the relaxation mechanism. Unlike the paramagnetic gradient diffusion phenomenon, this electron-nucleus dipolar relaxation effect does not depend on a sequestered intracellular compartment and shows the most pronounced lowering of water T_1 when the cells are lysed (Table 3).

The water relaxation times for whole blood have been analyzed and reported as single exponentials in all studies. Koivula et al. argued that the mono-exponential behavior was a consequence of the fast exchange of water on the T_1 time scale [42]. On first thought, this seems counterintuitive given that distinct intracellular and extracellular water compartments are separated by a cell membrane that is only selectively permeable to water. However, fast exchange is defined in relative terms. The T_1 time scale for whole blood can be estimated, in this case, by the difference in water relaxation times for isolated plasma and blood cells, approximately 600–800 msec (Table 3). The reported lifetime for the transmembrane exchange of water across the red blood cell membrane is much shorter, approximately 10 ms [73]. Moreover, T_1 values for whole blood samples diluted with their own plasma are linearly correlated with hemoglobin content, providing further evidence for the “fast” exchange of water across the red blood cell membrane [74].

Another factor to consider in the relaxation time analysis of whole blood is the spontaneous settling of blood cells in the NMR tube, which generates a cell pellet and plasma supernatant [66]. This process takes just a few minutes [63], well within the time often employed for pre-acquisition temperature equilibration and instrument calibration. Some investigators have devised special mixing tubes or flow perfusion systems to prevent cell settling and to mimic *in vivo* conditions [12,63,64,66,68]. However, other reports did not specify protocols for keeping blood samples mixed during analysis [58–60,62,75,76]. Sample settling could generate instrument-dependent artifacts that depend on sample geometry and rf coil design, with variation in the relative amounts of cell pellet and plasma supernatant exposed to the active range the transceiver coil. On the other hand, the fast exchange of water between compartments may attenuate or eliminate some of these artifacts. In any case, it is important to consider how sample settling may impact the data acquisition, analysis and interpretation.

The water T_1 relaxation times for whole blood and blood cells show a significant dependence on the B_o magnetic field strength [12,59,60]. For whole blood, T_1 values increase from approximately 1000 ms at 20 MHz, to 1400–1700 ms at 63.9 MHz; a similar increase is observed with isolated blood cells (Table 3). This trend is consistent with dipolar relaxation resulting from the rotational tumbling of water molecules, in rapid exchange between the protein-bound and unbound states. Dipolar relaxation becomes more efficient, and T_1 becomes shorter, as the rotational correlation rate approaches the Larmor frequency.

By contrast, the T_2 values for human blood do not show this B_o field dependence. As discussed above, additional exchange and diffusion effects are seen most vividly in deoxygenated blood or blood cell samples. The shortest T_2 values are observed in

deoxygenated samples collected with long 2τ values at higher B_o fields (Table 3 and refs. [59,60,67]).

Other factors, such as temperature, pH [38] and hematocrit [12,66] affect the T_1 and T_2 values of whole blood. Precautions to control sample pH by minimizing the release of CO_2 from the intrinsic bicarbonate buffer system have been discussed [38].

4.2. Blood relaxometry and human disease

Like plasma and serum, whole blood relaxation times are strongly influenced by protein content [42]. So it follows that blood T_1 and T_2 values may be potential biomarkers for changes in the total concentration and/or relative distribution of blood proteins. Hemoglobin is, by far, the most abundant single protein in *whole* blood, representing approximately two-thirds of the total blood protein concentration. Hemoglobin levels correlate strongly with red blood cell count and hematocrit, the volume percent of blood taken up by cells. Indeed, T_2 values are sensitive to hemoglobin and hematocrit [12,42,66,77]. So it is conceivable that T_1 and/or T_2 values could be used as markers for anemia.

Anemia is a low blood cell count, or low hemoglobin level, resulting from three main causes: low production, increased degradation, or blood loss. Low production can occur in aplastic anemia, cancer, lymphomas, iron deficiency, hypothyroidism and chronic kidney disease. Anemia was the likely underlying cause of the apparent association between increased blood T_1 and cancer observed in some studies [42,77]. Increased degradation can occur with splenomegaly, porphyria, thalassemia, vasculitis, and hemolysis. Blood loss can occur from wounds, gastro-intestinal, urinary or menstrual bleeding, or frequent blood donation. Anemia is routinely identified and evaluated using a complete blood count (CBC) [78].

If red cell abnormalities can be assessed with a routine CBC, then what added value could NMR relaxation time measurements bring to the clinical screening of anemia? The answer lies in the advantages of compact NMR relaxometry: portability, simplicity, cost. It is conceivable that portable NMR devices could be used to measure hematocrit and other blood cell abnormalities non-invasively. In real-world primary care or community settings, the feasibility of deploying new tests for population screening or front-line diagnosis often hinges on practical considerations like these.

Although red blood cells are the dominant cell type in whole blood, early studies by Ekstrand et al. compared the T_1 values for white blood cells (leukocytes) in normal individuals with those for individuals with various disease states [40]. The leukocyte T_1 values were higher in individuals with active leukemia, as well as in non-leukemic individuals who have elevated white blood cell counts or leukocytosis. While the clinical significance of this finding was not determined at that time, it is conceivable that the elevated T_1 values in leukocytosis are a characteristic of activated neutrophils, which function as a first line of defense against pathogens.

An exciting new application of compact NMR relaxometry to human blood pertains to a quick and label-free diagnosis of malaria [79]. The *Plasmodium* parasites that infect red

blood cells metabolize large amounts of hemoglobin and generate paramagnetic hemozoin crystallites. The resulting magnetic susceptibility differences lead to large changes in the water T_2 values of red blood cells. The compact NMR device designed for this work is illustrated in Fig. 5a. The changes in R_2 during repeated 48-hour life cycles of the malaria parasite are plotted in Fig. 5b [79].

5. Conclusions and future prospects

As cataloged in this review, a sizeable number of low-field and compact relaxometry studies have been carried out to define the basis for water relaxation in purified blood proteins, whole plasma and serum, fractionated blood cells and whole blood. These results have been steadily translated into improvements in magnetic resonance imaging that have dramatically enhanced image quality and diagnostic capabilities. Several applications of compact NMR relaxometry have been successfully translated into blood-based diagnostic tests for Candidiasis, malaria, and hemostasis, which signals that compact NMR relaxometry has begun to reach its stride in clinical chemistry and medicine.

Because water T_2 can monitor the net effect of shifts in the distribution of many proteins in the blood with just one measurement, it could be characterized as a method for inverse proteomics. Protein shifts of this type occur with inflammation – both the acute phase response to overt infection or injury, as well as the more subtle inflammation that may occur with nutrient imbalance and insulin resistance, an early predictor of prediabetes and diabetes. A significant opportunity lies in applying water T_2 to detect subtle forms of inflammation that are not detected by conventional diagnostic tests. Compact NMR relaxometry is sufficiently portable, simple and cost-effective to be translated into such applications.

The ultimate goal is to develop simple tests that require no blood. As water NMR signals from blood can be measured from outside the body, one can envision a compact NMR device designed to monitor human physiology.

Beyond medical and diagnostic applications, compact NMR relaxometry has untapped potential as an analytical tool. Much of the relaxometry performed to date has utilized mono-exponential analysis and has not exploited the intrinsic resolving power of T_2. For years, academic laboratories have focused on the use of mid-and high-field NMR spectroscopy to achieve resolution and address chemical problems. However, some problems or samples may lend themselves to compact relaxometry. Because of its portability, simplicity and low cost, compact NMR relaxometry should be appealing to wide range of chemists looking for a relatively simple and versatile analytical tool.

Acknowledgments

The authors thank Dr. Nate Bachman, Ina Mishra, Vipulkumar Patel, Kim Brown and Sneha Deodhar for helpful suggestions and assistance. This work was supported by pilot grants from the Garvey Texas Foundation, the East Carolina Diabetes & Obesity Institute, and institutional funds from the University of North Texas Health Science Center and East Carolina University.

References

1. Marcone MF, Wang S, Albabish W, Nie S, Somnarain D, Hill A. Food Res Int. 2013; 51:729.
2. Heaton N, Bachman HN, Minh CC, Decoster E, LaVigne J, White J, et al. Petrophysics. 2008; 49
3. Blumich B, Anferova S, Kremer K, Sharma S, Herrmann V, Sefre A. Spectroscopy (Springf). 2003; 18:18.
4. Danieli E, Blümich B. J Magn Reson. 2013; 229:142. [PubMed: 23290626]
5. Robinson MD, Cistola DP. Biochemistry. 2014; 53:7515. http://pubs.acs.org/doi/full/10.1021/bi5011859. [PubMed: 25409529]
6. James, TL. Anonymous Selected Topics in Biophysics. Biophysical Society; Rockville, MD: 1998. p. 1-31.http://www.Biophysics.Org/Portals/1/PDFs/Education/James.pdf
7. Freeman, R. A Handbook of Nuclear Magnetic Resonance. 2. Longman Group; United Kingdom: 1997.
8. Levitt, M. Spin Dynamics: Basics of Nuclear Magnetic Resonance. John Wiley & Sons, Ltd; New York, NY: 2001.
9. Steele RM, Korb JP, Ferrante G, Bubici S. Magn Reson Chem. 2015; doi: 10.1002/mrc.4220
10. Cavanagh, J.; Fairbrother, WJ.; Palmer, WG., III; Rance, M.; Skelton, NJ. Protein NMR Spectroscopy. 2. Elsevier; 2007.
11. Levitt MH, Freeman R. J Magn Reson. 1969; 33:473. (1979).
12. Johanna Silvennoinen M, Kettunen MI, Clingman CS, Kauppinen RA. Arch Biochem Biophys. 2002; 405:78. [PubMed: 12176060]
13. Ishima R, Torchia DA. Nat Struct Mol Biol. 2000; 7:740.
14. Carr HY, Purcell EM. Phys Rev. 1954; 94:630.
15. Provencher S. Comput Phys Commun. 1982; 35:229.
16. Goldin, A. 2006. www.softscientific.com/science/xpfit.html
17. Granwehr J, Roberts P. J Chem Theory Comput. 2012; 8:3473. [PubMed: 26592997]
18. Ghosh S, Keener KM, Pan Y. J Magn Reson. 2008; 191:226. [PubMed: 18221903]
19. Robinson MD, Deodhar S, Mishra I, Patel V, Gordon K, Vintimilla R, et al. Arterioscler Thromb Vasc Biol. 2015; 35:A620.
20. Lundblad R. Internet J Genom Proteom. 2003; 1(2)
21. Kang YS, Gore JC, Armitage IM. Magn Reson Med. 1984; 1:396. [PubMed: 6443783]
22. Raeymaekers HH, Borghys D, Eisendrath H. Magn Reson Med. 1988; 6:212. [PubMed: 2835571]
23. Schuhmacher JH, Conrad D, Manke HG, Clorius JH, Matys ER, Hauser H, et al. Magn Reson Med. 1990; 13:103. [PubMed: 2319928]
24. Yilmaz A, Ulak FS, Batun MS. Magn Reson Imaging. 2004; 22:683. [PubMed: 15172062]
25. Einstein, A. Investigations on the Theory of the Brownian Movement. Dover Publications; Mineola, New York: 1956. (re-publication of the original translation from 1926)
26. Debye, PJW. Polar Molecules. The Chemical Catalog Company, Inc; New York: 1929.
27. Venu K, Denisov VP, Halle B. J Am Chem Soc. 1997; 119:3122.
28. Hills BP. Mol Phys. 2006; 76:489.
29. Chen E, Kim RJ. PLoS ONE. 2010; 5:e8565. [PubMed: 20052404]
30. Koenig SH, Baglin CM, Brown RD 3rd. Magn Reson Med. 1985; 2:283. [PubMed: 3938511]
31. Grosch L, Noack F. Biochim Biophys Acta. 1976; 453:218. [PubMed: 999881]
32. Pouliquen D, Gallois Y. Biochimie. 2001; 83:891. [PubMed: 11698111]
33. Denisov VP, Halle B. J Mol Biol. 1995; 245:698. [PubMed: 7531249]
34. Denisov VP, Halle B. J Mol Biol. 1995; 245:682. [PubMed: 7531248]
35. Atkinson D, Deckelbaum RJ, Small DM, Shipley GG. Proc Natl Acad Sci USA. 1977; 74:1042. [PubMed: 191827]
36. Prassl R, Laggner P. Eur Biophys J. 2009; 38:145–158. [PubMed: 18797861]
37. Hamilton JA, Morrisett JD. Meth Enzymol. 1986; 128:472. [PubMed: 3724520]

38. McLachlan LA. Phys Med Biol. 1980; 25:309. [PubMed: 7384216]
39. Schuhmacher JH, Clorius JH, Semmler W, Hauser H, Matys ER, Maier-Borst W, et al. Magn Reson Med. 1987; 5:537. [PubMed: 3437814]
40. Ekstrand K, Dixon R, Raben M, Ferree C. Phys Med Biol. 1977; 22:925. [PubMed: 561969]
41. Beall, P.; Medina, D.; Hazlewood, C. Anonymous NMR in Medicine. Springer; 1981. p. 39-57.
42. Koivula A, Suominen K, Timonen T, Kiviniitty K. Phys Med Biol. 1982; 27:937. [PubMed: 7111398]
43. Beall PT, Narayana PA, Amtey SR, Spiga L, Intra E, Ridella S, et al. Magn Reson Imaging. 1984; 2:83. [PubMed: 6085132]
44. Damadian R. Science. 1971; 171:1151. [PubMed: 5544870]
45. Hollis DP, Economou JS, Parks LC, Eggleston JC, Saryan LA, Czeister JL. Cancer Res. 1973; 33:2156. [PubMed: 4725372]
46. Floyd RA, Leigh JS Jr, Chance B, Miko M. Cancer Res. 1974; 34:89. [PubMed: 4809464]
47. Hollis DP, Saryan LA, Economou JS, Eggleston JC, Czeisler JL, Morris HP. J Natl Cancer Inst. 1974; 53:807. [PubMed: 4370227]
48. Beall PT, Medina D, Chang DC, Seitz PK, Hazlewood CF. J Natl Cancer Inst. 1977; 59:1431. [PubMed: 909106]
49. Gangardt MG, Karyakina NF, Pavlov AS, Papish EA. Bull Exp Biol Med. 1995; 120:1179.
50. Gangardt MG, Popova OV, Shmarov DA, Kariakina NF, Papish EA, Kozinets GI. Klin Lab Diagn. 2002; 8:23.
51. Hotamisligil GS, Erbay E. Nat Rev Immunol. 2008; 8:923. [PubMed: 19029988]
52. Romeo GR, Lee J, Shoelson SE. Arterioscler Thromb Vasc Biol. 2012; 32:1771. [PubMed: 22815343]
53. Guariguata L, Whiting DR, Hambleton I, Beagley J, Linnenkamp U, Shaw JE. Diabetes Res Clin Pract. 2014; 103:137. [PubMed: 24630390]
54. DeFronzo RA, Abdul-Ghani MA. J Clin Endocrinol Metab. 2011; 96:2354. [PubMed: 21697254]
55. Neely LA, Audeh M, Phung NA, Min M, Suchocki A, Plourde D, et al. Sci Transl Med. 2013; 5
56. Pfaller MA, Wolk DM, Lowery TJ. Future Microbiol. 2016; 11:103. [PubMed: 26371384]
57. Skewis LR, Lebedeva T, Papkov V, Thayer EC, Massefski W, Cuker A, et al. Clin Chem. 2014; 60:1174. [PubMed: 24958814]
58. Thulborn KR, Waterton JC, Matthews PM, Radda GK. Biochim Biophys Acta. 1982; 714:265. [PubMed: 6275909]
59. Gomori JM, Grossman RI, Yu-Ip C, Asakura T. J Comput Assist Tomogr. 1987; 11:684. [PubMed: 3597895]
60. Bryant RG, Marill K, Blackmore C, Francis C. Magn Reson Med. 1990; 13:133. [PubMed: 2319929]
61. Matwiyoff NA, Gasparovic C, Mazurchuk R, Matwiyoff G. Magn Reson Imaging. 1990; 8:295. [PubMed: 2366641]
62. Wright GA, Hu BS, Macovski A. J Magn Reson Imaging. 1991; 1:275. [PubMed: 1802140]
63. Gasparovic C, Matwiyoff NA. Magn Reson Med. 1992; 26:274. [PubMed: 1325024]
64. Meyer ME, Yu O, Eclancher B, Grucker D, Chambron J. Magn Reson Med. 1995; 34:234. [PubMed: 7476083]
65. Gillis P, Peto S, Moiny F, Mispelter J, Cuenod CA. Magn Reson Med. 1995; 33:93. [PubMed: 7891542]
66. Spees WM, Yablonskiy DA, Oswood MC, Ackerman JJH. Magn Reson Med. 2001; 45:533. [PubMed: 11283978]
67. Silvennoinen MJ, Clingman CS, Golay X, Kauppinen RA, van Zijl PC. Magn Reson Med. 2003; 49:47. [PubMed: 12509819]
68. Stefanovic B, Pike GB. Magn Reson Med. 2004; 52:716. [PubMed: 15389952]
69. Ogawa S, Lee TM, Kay AR, Tank DW. Proc Natl Acad Sci USA. 1990; 87:9868. [PubMed: 2124706]
70. Yablonskiy DA, Sukstanskii AL, He X. NMR Biomed. 2013; 26:963. [PubMed: 22927123]

71. Kim SG, Ogawa S. J Cereb Blood Flow Metab. 2012; 32:1188. [PubMed: 22395207]
72. Thulborn KR. Neuroimage. 2012; 62:589. [PubMed: 22001265]
73. Herbst MD, Goldstein JH. Am J Physiol. 1989; 256:C1097. [PubMed: 2719098]
74. Yilmaz A, Hamamci C. Spectrosc Lett. 1990; 23:349.
75. Brooks RA, Di Chiro G. Med Phys. 1987; 14:903. [PubMed: 3696078]
76. Barth M, Moser E. Cell Mol Biol (Noisy-Le-Grand). 1997; 43:783. [PubMed: 9298600]
77. Yilmaz A, Tez M, Degertekin H. Spectrosc Lett. 1989; 22:925.
78. Ford J. Int J Lab Hematol. 2013; 35:351.doi: 10.1111/ijlh.12082 [PubMed: 23480230]
79. Peng WK, Kong TF, Ng CS, Chen L, Huang Y, Bhagat AA, et al. Nat Med. 2014; 20:1069. [PubMed: 25173428]
80. Pintaske J, Martirosian P, Graf H, Erb G, Lodemann KP, Claussen CD, et al. Invest Radiol. 2006; 41:213. [PubMed: 16481903]
81. Rohrer M, Bauer H, Mintorovitch J, Requardt M, Weinmann HJ. Invest Radiol. 2005; 40:715. [PubMed: 16230904]

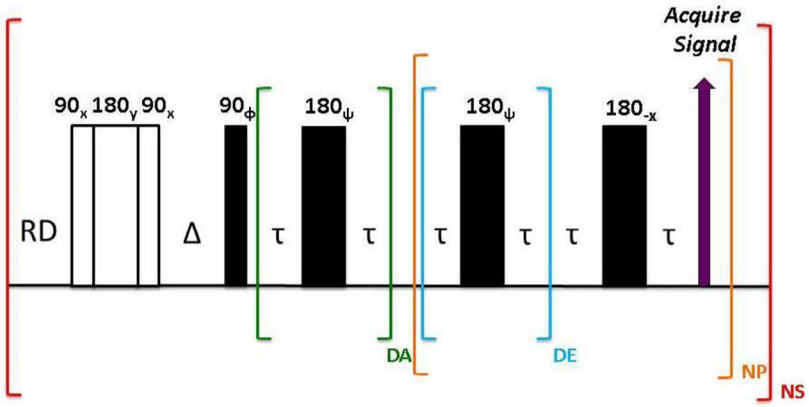

Fig. 1.

Modified Carr-Purcell-Meiboom-Gill (CPMG) pulse sequence for measuring T_2 in human blood serum or plasma using benchtop time-domain NMR relaxometry. The key elements of the pulse sequence are discussed in the text. For a 10 mm tube, the Δ delay is tuned to $0.95*T_1$, which corresponds to suppression of the water to 23% of its full intensity. For samples in a co-axial insert within a 10 mm tube, the composite 180 and delta delay are disabled. The τ delay is kept short (0.19 ms) to minimize the possible impact of translational diffusion on T_2 in an inhomogeneous B_o field. The green loop utilizes DA = 42 to achieve delayed acquisition of the first data point until after the first 19 ms of intensity decay. With DE = 5, the signal intensity of one in every six echoes was recorded during the NP loop. In contrast to conventional NMR spectroscopy, the time points for the exponential decay curve are recorded directly during the CPMG pulse scheme, as designated by the purple arrow. The relaxation delay RD was set to $5*T_1$, corresponding to ~8 sec for serum or plasma; NP = 5600, NS = 8. Phase cycles for the pulses: $\varphi = (x)_2, (-x)_2, (y)_2, (-y)_2$; $\psi = x,-x$. Phase cycle of the receiver: same as φ. Total experiment time for 8 scans: 3.2 minutes. Data were recorded at 37°C using a Bruker Minispec mq20 operating at 0.47T (20MHz for ^1H).

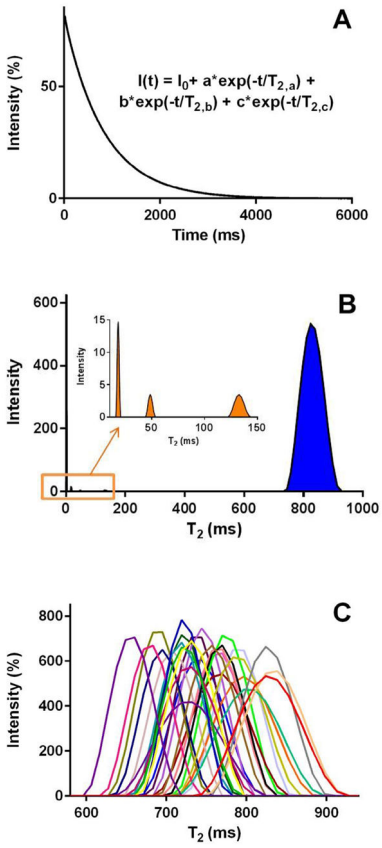

Fig. 2.

Time-domain NMR relaxometry analysis of human blood serum. (A) Raw NMR relaxometry data for human serum consisting of a multi-exponential CPMG decay curve; (B) CONTIN-generated T_2 profile for human serum, derived from a continuous inverse Laplace transform of the multi-exponential decay curve in (A). This profile is not to be confused with a conventional NMR spectrum. The T_2 profile reveals an intense water peak (blue) and a few small peaks arising from directly-detected lipid and protein components of serum (orange). (C) Expansions of the water T_2 profiles for individual human subjects illustrating the wide range of T_2 values observed across a cohort of 29 presumably healthy human subjects. Panel C is reproduced from ref. [19], with permission from Wolters Kluwer Health, Inc.

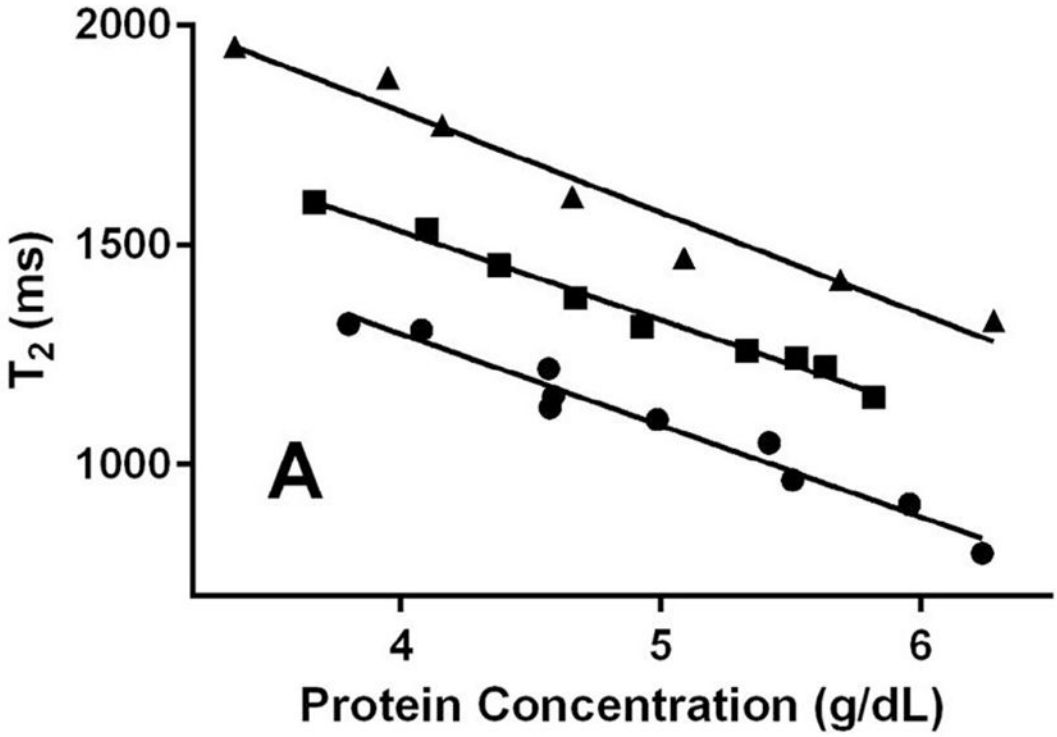

Fig. 3.

Variation of water T_2 values with total protein concentration for samples of human serum albumin (▲), lipoprotein-depleted human serum (■) and whole human serum (●). The whole serum and lipoprotein-deficient serum samples were progressively diluted with phosphate-buffered saline to in order to vary total protein concentration. Similarly, a concentrated albumin stock solution was progressively diluted. Total protein concentrations were determined using the bicinchoninic (BCA) assay, as implemented in a kit from the Pierce Protein Biology Division of Thermo Fisher Scientific.

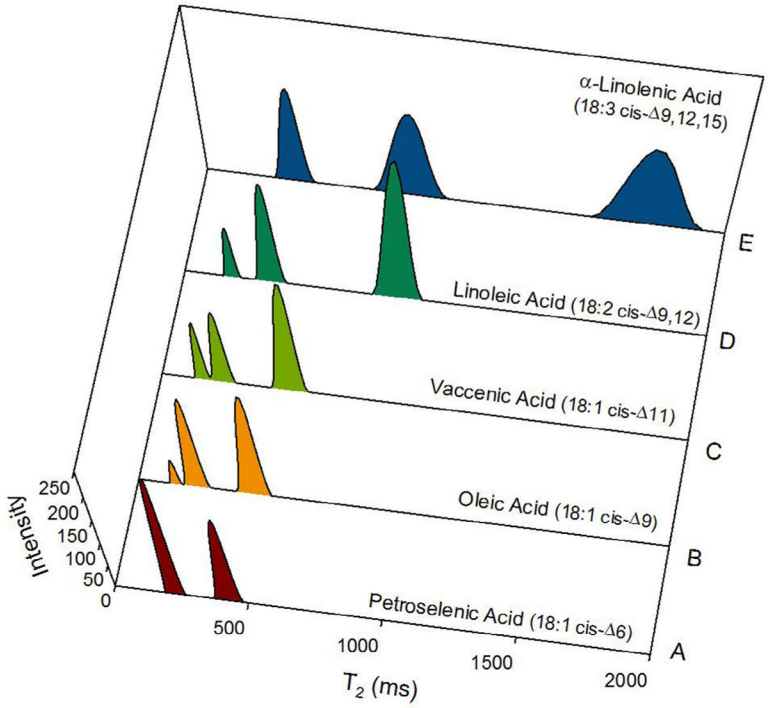

Fig. 4.

T_2 profiles for 18-carbon *cis*-unsaturated fatty acids at 37°C: Effect of double bond position and number. (A) Petroselenic acid, 18:1 *cis*-Δ^6; (B) Oleic acid, 18:1 *cis*-Δ^9; (C) Vaccenic acid, 18:1 *cis*-Δ^{11}; (D) Linoleic acid, 18:2 *cis*-$\Delta^{9,12}$; (E) α-Linolenic acid, 18:3 *cis*-$\Delta^{9,12,15}$. The addition of *cis* double bonds causes large increases in the T2 values for resolved lipid mobility domains. This figure was reproduced from reference [5], and used by permission from the American Chemical Society.

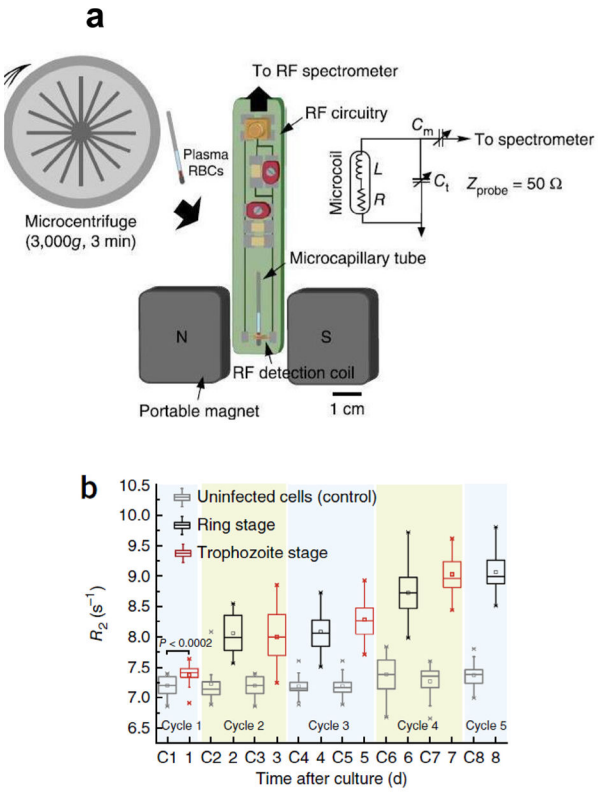

Fig. 5.

Relaxometry-based method for the rapid detection of malaria parasite-infected red blood cells in whole blood, from reference [79]. The parasite is detected by its production of hemozoin, which creates magnetic susceptibility differences and T_2 changes for red blood cells. (a) Schematic illustration of the compact NMR relaxometry system, which consists of a portable permanent magnet that provides a strong polarizing magnetic field and a home-built radiofrequency (RF) detection probe. The bio-sensor is connected to an RF unit, which acts as a transmitter and receiver of the RF signal. A micro centrifuge is used to separate the plasma from the RBC- and iRBC-containing pellet inside a microcapillary tube. The microcapillary tube is then slotted into the RF detection probe. The RF circuitry (right) of the detection probe (50 Ω impedance) was tuned to the resonance frequency for protons (21.65 MHz) using variable capacitance at Cm = 40 pF and Ct = 800 pF. L, inductance; R, resistance of the coil; C, capacitance of the circuit. (b) *P. falciparum* (malaria parasite) infection and the R_2 responses as measured by the NMR relaxometry system. The 48-h life cycle of *P. falciparum* inside red blood cells is such that the hemozoin pigment becomes more prominent as the cell cycle proceeds into the later stages. This R_2 increases as the cycle progresses, and the cultures are synchronized every 48 hours. The box plots show the lower quartile, median and upper quartile of their respective sample distributions. The control reading (gray boxplots) is denoted as C1 to C8 for its respective days. An 2τ inter-echo time of 200 μs, consisting of 2000 echoes, a total of 24 scans, was used. 10 samplings were taken per time point in every 24 h throughout the experiment. R_2 index for post-infection cycle 1 was significantly higher than healthy baseline ($P < 0.0002$), determined by

two-tailed Student's *t*-test. The figures and legends were adapted from reference [79] and used by permission from the Nature Publishing Group.

Table 1

^{1}H T_1 and T_2 Water Relaxivity Values for Human Blood Components $(s*g/dL)^{-1}$

Protein	R_{T2}	R_{T1}	R_{T2}/R_{T1}	B_o field	Sample Temp.	Ref.
Serum albumin	0.15	0.053	2.9	20 MHz	37°C	[21]
	0.24	0.035	6.9	42.6 MHz	ambient	[24]
	–	0.059	–	10.7 MHz	7°C	[22]
γ-globulin fraction	0.68	0.045	15	42.6 MHz	ambient	[24]
	–	0.053	–	10.7 MHz	7°C	[22]
α-globulin fraction	0.60	0.060	10	42.6 MHz	ambient	[24]
α + β fraction	0.46	0.052	8.9	42.6 MHz	ambient	[24]
	–	0.101	–	10.7 MHz	7°C	[22]
γ + β fraction	0.30	0.080	3.8	42.6 MHz	ambient	[24]
Albumin + γ-globulin	0.29	0.069	4.2	20 MHz	37°C	[21]
Fibrinogen	0.50	0.03	16.7	42.6 MHz	ambient	[24]
Transferrin	2.6	2.4	1.1	42.6 MHz	ambient	[24]
Diluted whole serum	0.38	0.042	9	42.6 MHz	ambient	[24]

Trends Analyt Chem. Author manuscript; available in PMC 2016 December 19.

Table 2

Water ^{1}H Relaxation Times for Human Blood Plasma and Serum

Sample	T_1 (msec)	T_2 (msec)	Exp. Conditions[a]	Physiological Conditions	Ref.
Plasma	1250 ± 10	357 ± 5	8.5 MHz, 22°C	2 healthy subjects, pooled[b]	[80]
Plasma	1410 ± 80[c]	–	19.8 MHz, 33°C	20 healthy subjects[b]	[42]
Plasma	1560 ± 170[c]	–	19.8 MHz, 33°C	18 blood cancer patients[b]	[42]
Plasma	1765 ± 63[d]	761 ± 54[e]	20.0 MHz, 37°C	19–23 fasting, healthy subjects[f]	[19]
Plasma	1440	490	20.0 MHz, 37°C	1 healthy subject[b]	[21]
Plasma	1481 ± 50[g]	565 ± 35[g]	20.0 MHz, 25°C	30 healthy subjects[b]	[38]
Plasma	1429 ± 102[g]	476 ± 91[g]	20.0 MHz, 25°C	6 leukemia patients[b]	[38]
Plasma	1563 ± 95[g]	595 ± 57[g]	20.0 MHz, 25°C	27 cancer patients[b]	[38]
Plasma	1460 ± 81[g]	526 ± 55[g]	20.0 MHz, 25°C	120 “other” diseases[b]	[38]
Plasma	1418 ± 60	689 ± 45	20.0 MHz, 20°C	28 healthy subjects[h]	[23]
Plasma	1414 ± 60	627 ± 86	20.0 MHz, 20°C	27 patients with lung diseases[i]	[23]
Plasma	1397 ± 50	589 ± 81	20.0 MHz, 20°C	22 patients with lung infections[j]	[23]
Plasma	1402 ± 60	593 ± 74	20.0 MHz, 20°C	50 patients with lung cancers	[23]
Plasma	1417 ± 90	592 ± 85	20.0 MHz, 20°C	15 patients w/lung metastases	[23]
Plasma	1499 ± 7	530 ± 2	20.0 MHz, 40°C	not specified	[81]
Plasma	1260 ± 60	–	24.0 MHz, 22°C	healthy, unspecified number	[40]
Plasma	1105 ± 100	–	24.0 MHz, 22°C	leukemia, unspecified number	[40]
Plasma	1280 ± 70	–	24.0 MHz, 22°C	cervical cancer, unspecified no.	[40]
Plasma	1780 ± 20	–	35.0 MHz, 45°C	healthy, unspecified number[k]	[50]
Plasma	1700 ± 60	–	35.0 MHz, 45°C	anemia, unspecified number[k]	[50]
Plasma	1970 ± 480	–	35.0 MHz, 45°C	leukocytosis, unspecified[k]	[50]
Plasma	2400 ± 120	–	35.0 MHz, 45°C	2nd/3rd deg burns, unspecified[k]	[50]
Plasma	2000 ± 10	400 ± 10	42.6 MHz, 22°C	2 healthy subjects, pooled	[80]
Plasma	2041 ± 173	500 ± 50	63.9 MHz, 37°C	not specified	[66]
Plasma	~1200[l]	–	14.9 MHz, 20°C	not specified	[59]

Sample	T_1 (msec)	T_2 (msec)	Exp. Conditions[a]	Physiological Conditions	Ref.
Plasma	~1500[l]	–	30.2 MHz, 20°C	not specified	[59]
Plasma	~1700[l]	–	40.0 MHz, 20°C	not specified	[59]
Plasma	~1700[l]	–	59.6 MHz, 20°C	not specified	[59]
Serum	1735 ± 69[m]	812 ± 51[n]	20.0 MHz, 37°C	23 healthy subjects, 12-h fast[e]	[19]
Serum	906 ± 50	–	10.7 MHz, 7°C	30 healthy subjects	[22]
Serum	–	742 ± 67	20.0 MHz, 20°C	8 healthy subjects	[23]
Serum	1230 ± 170	–	24.0 MHz, 22°C	healthy, unspecified number	[40]
Serum	1170 ± 100	–	24.0 MHz, 22°C	leukemia (remission), unspecified	[40]
Serum	1230 ± 90	–	24.0 MHz, 22°C	cervical cancer, unspecified no.	[40]
Serum	1260 ± 80	–	24.0 MHz, 22°C	breast cancer, unspecified no.	[40]

[a] A B_O field strength of 1.0 Tesla corresponds to a ^1H resonance frequency of 42.58 MHz.

[b] Fasting status not specified.

[c] Mean ± S.D. for subject population; $P < 0.001$ for healthy *vs.* blood cancer patients.

[d] Mean ± S.D. for 19 subjects following a 12-hour overnight fast; healthy as defined in footnote f.

[e] Mean ± S.D. for 23 subjects following a 12-hour overnight fast; healthy as defined in footnote f.

[f] This healthy cohort excluded individuals with a documented diagnosis of diabetes or a current HbA_1c level ≥6.5, those with a recent infection or injury or a *hs*-CRP level >10, and those with insulin resistance (fasting insulin > 12).

[g] Mean ± S.D. for subject population.

[h] Subjects were non-fasting.

[i] Lung diseases: chronic bronchitis, asthma, sarcoidosis, emphysema and pleural effusion.

[j] Lung infections: tuberculosis and pneumonia.

[k] Article in Russian; data extracted from English abstract.

[l] Data estimated from graph.

[m] Mean ± S.D. for 18 healthy subjects, as defined in footnote f.

[n] Mean ± S.D. for 22 healthy subjects, as defined in footnote f.

Table 3

Water ^{1}H Relaxation Times for Human Blood Cells and Whole Blood

Sample	T_1 (msec)	T_2 (msec)	Exp. Conditions	Physiological Conditions	Ref.
Blood cells	590 ± 60[a]	–	19.8 MHz, 37°C	20 healthy subjects	[42]
Blood cells	720 ± 120[a]	–	19.8 MHz, 37°C	19 blood cancer subjects	[42]
Cells (lysed)	~1100[b]	~230[b]	59.6 MHz, 20°C[c]	HbO_2 = 100%	[37]
Cells (intact)	~1200[b]	~210[b]	59.6 MHz, 20°C[d]	HbO_2 = 100%	[37]
Cells (lysed)	~600[b]	~230[b]	59.6 MHz, 20°C[c]	HbO_2 = 0%	[37]
Cells (intact)	~1200[b]	~140[b]	59.6 MHz, 20°C[d]	HbO_2 = 0%	[37]
Cells (intact)	~1200[b]	~60[b]	59.6 MHz, 20°C[e]	HbO_2 = 0%	[37]
Blood cells	879	–	60 MHz, 20°C	6 healthy, pooled	[68]
Whole blood			FFC/Variable,	Bryant	[38]
Whole blood	900 ± 90[a]	–	19.8 MHz, 33°C	20 healthy subjects	[49]
Whole blood	1100 ± 160[a]	–	19.8 MHz, 33°C	35 blood cancer subjects	[49]
Whole blood	1040	265	20 MHz, 37°C	1 healthy subject	[21]
Whole blood	1020–1124	167–200	63.9 MHz, 22°C	4 healthy subjects	[45]
Whole blood	–	250	63.9 MHz, 22°C	5 healthy; HbO_2 = 96%	[40]
Whole blood	–	30	63.9 MHz, 22°C	5 healthy; HbO_2 = 30%	[40]
Whole blood	1434 ± 48	181 ± 23	63.9 MHz, 23°C	9 healthy subjects	[54]
Whole blood	1429 ± 20	~170	63.9 MHz, 37°C	not specified; HCT ~ 0.4	[43]
Whole blood	1695 ± 29	~220	63.9 MHz, 37°C	not specified; HCT ~ 0.3	[43]
Whole blood	1250 ± 156	227 ± 10	63.9 MHz, 37°C	not specified	[66]

[a] Mean ± S.D. for subject population; $P < 0.001$ for healthy *vs.* blood cancer patients

[b] Data estimated from graph.

[c] Delay between 180 pulses in CPMG (2τ) was varied from 2 to 32 ms.

[d] Delay between 180 pulses in CPMG, 2τ = 2 ms.

[e] Delay between 180 pulses in CPMG, 2τ = 32 ms.

Trends Analyt Chem. Author manuscript; available in PMC 2016 December 19.